Sensitivity of Torque Control for Seven-phase BLDC Machine with One Opened Phase under Constraints on Voltage and Current

Duc Tan Vu, Ngac Ky Nguyen, Eric Semail

Univ. Lille, Arts et Metiers ParisTech, Centrale Lille, HEI, EA 2697 - L2EP -Laboratoire d'Electrotechnique et d'Electronique de Puissance, F-59000 Lille, France

E-mail: {ductan.vu; ngacky.nguyen; eric.semail}@ensam.eu

Abstract- **This paper deals with control strategies when a seven-phase axial-flux brushless DC machine operates in one open-circuited phase fault by considering constraints on voltage and current. The constraints are related to the converter and machine design in terms of peak values of non-sinusoidal voltage and current. In addition, the sensitivity of the torque control on parameters of new imposed current references is analyzed under the base speed and in the flux-weakening region. The current references taking into account only first and third harmonics in healthy phases are proposed to ensure the torque optimization while phase currents and voltages are within their limits. The usefulness of the control strategies and the parameter analysis are verified by numerical results.**

Keywords- 7-phase BLDC machine; open-phase fault; fault-tolerant control; parameter sensitivity; torque control; constraints on non-sinusoidal voltage and current; flux-weakening.

I. INTRODUCTION

Multiphase machines have been utilized in variable-speed applications for a half of century and a significant rise in this area has been recorded in recent years because of the developments in some specific uses [1] and thanks to the advent of powerful processors. The design, modeling and control methods in healthy mode of operation are analyzed in [2]. One main advantage of multiphase machines is to have better fault-tolerance from faults of the power converter in comparison with their 3-phase counterparts [3, 4]. There is a variety of studies concerning open-circuited faults in the operation of multiphase machines. A constant torque can be obtained by a reconfiguration of control if the types of faults are detected and localized by a methodology as proposed in [5]. Many strategies have been proposed to determine optimal current references to maximize torque with a given copper loss level when one or more phases of the machines are open-circuited.

In [6-8], the fundamental and third harmonic current components for the excitation in healthy stator phases are introduced to control five-phase permanent-magnet motors with trapezoidal back-EMFs in open-phase faults. In these studies, there are eight unknown variables in current expressions that need to be determined (for example by Fmincon in MATLAB). By this way, machines with seven or more phases need more variables, which makes current solutions more complicated and

less accurate because optimization algorithms are usually sensitive to the number of variables. In [9], fault tolerant control strategies for a 7-phase machine using a vectorial multiphase description are verified with single and double open-circuit faults. However, these approaches have not considered the constraints on voltage and current of the drive system. These constraints play an important role in the sizing and cost of VSI as well as for the machine protection from thermal point of view. Besides, for wide speed-range applications such as electric vehicles or wind turbines, it is notable to take a flux-weakening strategy into account in the systems to meet the requirement of machine-converter voltage limits. In [10], a variable speed control method including voltage and current limits is applied to a 5-phase permanent magnet synchronous generator but with sinusoidal back-EMFs only. In [11], the authors have proposed different control strategies for odd and even phase sinusoidal machines in one opened-phase faults. New current references for the degraded modes ensure the same magnetomotive force (MMF) as in healthy mode. However, these methods are only for sinusoidal back-EMF machines and the issue on maximum currents and voltages have not been considered. In [12], an interesting approach is proposed, for 5-phase sinusoidal back-EMF machines, by defining a weighting factor which either optimizes copper losses in healthy operation or limits phase currents satisfying a required torque in case of one open-circuit faults, including the flux-weakening operation. However, the currents obtained by this approach contain high frequency components which limit the range of speed.

In this paper, based on [11], control strategies for one opened-phase fault is proposed to control the 7-phase brushless DC axial-flux machine with double identical rotors. The first and third harmonics of back-EMF are considered; therefore, the first and third harmonic currents are imposed to generate the torque. Simpler new current references are proposed with only three variables in the operation under base speed (with the control method of maximum torque per ampere (MTPA)) and four variables in the flux-weakening operation. Impacts of these variables are analyzed to optimize the mean torque amplitude and minimize the torque ripple while satisfying the constraints on peak values of non-sinusoidal current and voltage of the system, including flux-weakening region.
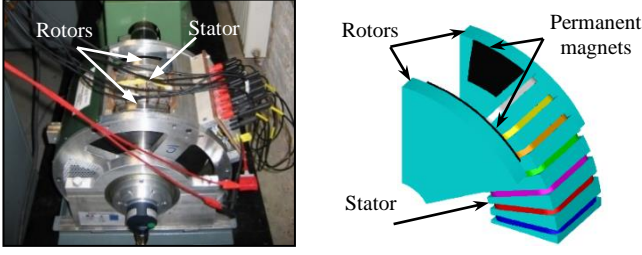
Fig. 1. The 7-phase axial-flux double rotor BLDC machine.

The paper is organized as follows: Section 2 describes the model and parameters of the considered machine. The control strategy in a single open-circuit fault is demonstrated in Section 3. Section 4 analyzes the impacts of variations in the current parameters on the torque production.

II. MULTI-PHASE MACHINE MODELING AND PARAMETERS

The design of the 7-phase BLDC machine is proposed in [13, 14] with axial flux and double identical rotors as shown in Fig. 1. To identify the machine model, these following assumptions are considered: 7 phases are equally shifted and wye-connected; the machine has trapezoidal back-EMFs; the saturation of the magnetic circuits is not taken into account in the calculation of the back-EMFs and fluxes.

The voltage vector and torque can be written as follows:

$$\vec{v} = R\vec{\imath} + \Lambda \frac{d\vec{\imath}}{dt} + \vec{e} \tag{1}$$

$$T_m = \frac{\vec{e}.\vec{\imath}}{\Omega} = \vec{e}_n.\vec{\imath} \tag{2}$$

where $\vec{v}$, $\vec{\imath}$ and $\vec{e}$ are the 7-dimensional stator voltage, current and back-EMF vectors respectively; R is the stator resistance of each phase; Λ is a 7 by 7 stator inductance matrix; T_m is the torque and Ω is the rotating speed of the machine; $\vec{e}_n = (e_{an}, e_{bn}, e_{cn}, e_{dn}, e_{en}, e_{fn}, e_{gn})$ is the speed-normalized back-EMF vector.

In fact, the speed-normalized back-EMFs of the machine contain many harmonics as expected by analyzing Fig. 2. The RMS values of the first and third harmonics account for the highest proportions while those of higher harmonics can be neglected [9]. For simplicity of current and torque expressions, the back-EMFs are assumed to contain only the first and third harmonics as expressed in equation (3).

$$e_{jn} = E_{m1}sin\left(\omega t - (j-1)\frac{2\pi}{7}\right) + E_{m3}sin\left(3\left(\omega t - (j-1)\frac{2\pi}{7}\right)\right) \tag{3}$$

where e_{jn} is the speed-normalized back-EMF of phase j; E_{m1}, E_{m3} and $k_e = E_{m3}/E_{m1}$ are the amplitudes and the ratio of the first and third harmonics of the back-EMF respectively; $\omega = p\Omega$ is the electric speed of the machine.

The electrical parameters of the 7-phase machine and converter for validating the efficiency of the control strategies and analyzing the sensitivity of current parameters are shown in Table 1.

TABLE I. ELECTRICAL PARAMETERS OF CONVERTER AND MACHINE

Parameter	Value
Stator resistance R (Ω)	1.4
Phase inductance L (mH)	10.1
Mutual inductance M_1 (mH)	3.1
Mutual inductance M_2 (mH)	-1.05
Mutual inductance M_3 (mH)	-5.3
Number of pole pairs p	3
Speed-normalized amplitude of 1st harmonic back-EMF E_{m1} (V/rad/s)	2.38
Speed-normalized amplitude of 3rd harmonic back-EMF E_{m3} (V/rad/s)	0.45
DC bus voltage V_{DC} (V)	200
Maximum peak current (A)	7.5

In this machine, the amplitude of the third harmonic back-EMFs equals approximately 19% of the first harmonic ones ($k_e = E_{m3}/E_{m1} = 0.19$). The converter is supplied by a DC bus voltage of 200 V and the allowed peak phase current is 7.5 A.

III. CONTROL METHOD IN DEGRADED MODE

Without loss of generality, it can be assumed that the open-circuited fault happens in phase a. The control strategy is adapted for other open-circuited phases. When one phase is open-circuited, it is necessary to keep continuous operations of the drive with acceptable performances. However, the imposed current references in healthy mode are often unsuitable for the faulty cases in some applications such as offshore wind energy systems due to mechanical resonance created by torque ripples; therefore, these currents need to be modified [9]. In [11], the authors have proposed new sinusoidal current references for healthy phases of sinusoidal back-EMF seven-phase machines in a single opened-phase fault. These sinusoidal currents are assumed to have the same amplitude which is, for the same torque, 23% higher than in normal operation. Nevertheless, the constraints on current and voltage and methods for trapezoidal back-EMF machines have not been considered.

In this paper, new non-sinusoidal current references for the non-sinusoidal back-EMF seven-phase machine are proposed. The first and third harmonic currents are considered to contribute to the torque production. The new current references in the natural frame are denoted by $i'_b, i'_c, i'_d, i'_e, i'_f$ and i'_g and expressed by equations (4-9).

$$i'_b = I_{m1}sin(\omega t + \varphi_b + \varphi_1) + I_{m3}sin\left(3(\omega t + \varphi_b + \varphi_3)\right) \tag{4}$$

$$i'_c = I_{m1}sin(\omega t + \varphi_c + \varphi_1) + I_{m3}sin\left(3(\omega t + \varphi_c + \varphi_3)\right) \tag{5}$$

$$i'_d = I_{m1}sin(\omega t + \varphi_d + \varphi_1) + I_{m3}sin\left(3(\omega t + \varphi_d + \varphi_3)\right) \tag{6}$$

$$i'_e = -i'_b \tag{7}$$

$$i'_f = -i'_c \tag{8}$$

$$i'_g = -i'_d \tag{9}$$

$$T = I_{m1}E_{m1}\left\{\begin{array}{l}\left(k_1cos\left(\omega t - \frac{5\pi}{7}\right) + k_3cos\left(3\left(\omega t - \frac{5\pi}{7}\right)\right)\right)\left(sin(\omega t + \varphi_b + \varphi_1) + k_i sin(3(\omega t + \varphi_b + \varphi_3))\right) \\ -\left(k_1cos(\omega t) + k_3cos(3(\omega t))\right)\left(sin(\omega t + \varphi_c + \varphi_1) + k_i sin(3(\omega t + \varphi_c + \varphi_3))\right) \\ +\left(k_1cos\left(\omega t - \frac{9\pi}{7}\right) + k_3cos\left(3\left(\omega t - \frac{9\pi}{7}\right)\right)\right)\left(sin(\omega t + \varphi_d + \varphi_1) + k_i sin(3(\omega t + \varphi_d + \varphi_3))\right)\end{array}\right\} \quad (10)$$

where I_{m1} and I_{m3} are the amplitudes of the first and third harmonic currents respectively; φ_b, φ_c and φ_d are constant initial phase angles of phase b, c and d respectively, determined by the method in [11]; φ_1 and φ_3 are adjustable phase angles of the first and third harmonics of currents.

The proposed current references with the same amplitude enable an equal distribution of copper losses in all healthy phases of the machine. Hence, the requirements of the machine design are significantly simplified. The above references also satisfy the assumption of the wye connection because the sum of all instantaneous currents is zero. Besides, the waveform of current in each phase with MTPA control is like the corresponding experimental back-EMF as shown in Fig. 2. This similarity allows the machine to obtain the maximum torque.

From equations (2-9), the generated torque could be expressed in equation (10) in which $k_1 = 2sin(3\pi/7)$ and $k_3 = 2k_e sin(9\pi/7)$ are constants determined from the machine parameters; $k_i = I_{m3}/I_{m1}$ is the ratio between the third and first harmonics of the currents. The torque-time and torque-speed characteristics are functions of I_{m1}, k_i, φ_1 and φ_3. Adjustments of these parameters result in changes in the average torque and torque pulsation of the machine. This study investigates the impacts of these parameters on: the torque (average and ripple values), the speed range, the maximal values of current and voltage.

Additionally, the limits on voltage and current of the machine are shown in equations (11-12) and the absolute values of phase voltages are calculated as in equations (13-18).

$$\left[|i_b'|; |i_c'|; |i_d'|; |i_e'|; |i_f'|; |i_g'|\right] \le I_{max} \quad (11)$$

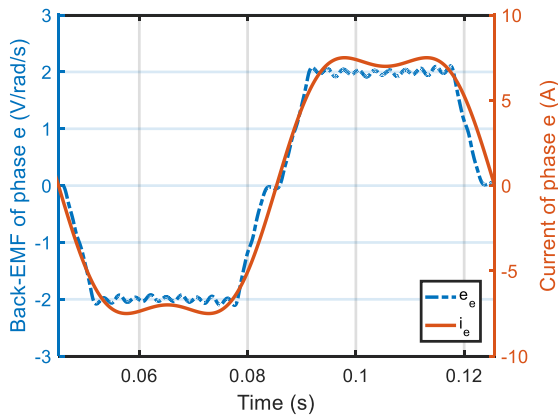$$\left[|v_b'|; |v_c'|; |v_d'|; |v_e'|; |v_f'|; |v_g'|\right] \le V_{max} \quad (12)$$

Fig. 2. Current reference with MTPA control and experimental back-EMF in phase e of the machine at 26 rad/s.

$$|v_b'| = \left|\begin{array}{l}Ri_b' + L\frac{di_b'}{dt} + M1\left(\frac{di_c'}{dt}\right) \\ +M2\left(\frac{di_d'}{dt} + \frac{di_g'}{dt}\right) + M3\left(\frac{di_e'}{dt} + \frac{di_f'}{dt}\right) + e_b\end{array}\right| \quad (13)$$

$$|v_c'| = \left|\begin{array}{l}Ri_c' + L\frac{di_c'}{dt} + M1\left(\frac{di_b'}{dt} + \frac{di_d'}{dt}\right) \\ +M2\left(\frac{di_e'}{dt}\right) + M3\left(\frac{di_f'}{dt} + \frac{di_g'}{dt}\right) + e_c\end{array}\right| \quad (14)$$

$$|v_d'| = \left|\begin{array}{l}Ri_d' + L\frac{di_d'}{dt} + M1\left(\frac{di_c'}{dt} + \frac{di_e'}{dt}\right) \\ +M2\left(\frac{di_b'}{dt} + \frac{di_f'}{dt}\right) + M3\left(\frac{di_g'}{dt}\right) + e_d\end{array}\right| \quad (15)$$

$$|v_e'| = \left|\begin{array}{l}Ri_e' + L\frac{di_e'}{dt} + M1\left(\frac{di_d'}{dt} + \frac{di_f'}{dt}\right) \\ +M2\left(\frac{di_c'}{dt} + \frac{di_g'}{dt}\right) + M3\left(\frac{di_b'}{dt}\right) + e_e\end{array}\right| \quad (16)$$

$$|v_f'| = \left|\begin{array}{l}Ri_f' + L\frac{di_f'}{dt} + M1\left(\frac{di_e'}{dt} + \frac{di_g'}{dt}\right) \\ +M2\left(\frac{di_d'}{dt}\right) + M3\left(\frac{di_c'}{dt} + \frac{di_b'}{dt}\right) + e_f\end{array}\right| \quad (17)$$

$$|v_g'| = \left|\begin{array}{l}Ri_g' + L\frac{di_g'}{dt} + M1\left(\frac{di_f'}{dt}\right) \\ +M2\left(\frac{di_b'}{dt} + \frac{di_e'}{dt}\right) + M3\left(\frac{di_c'}{dt} + \frac{di_d'}{dt}\right) + e_g\end{array}\right| \quad (18)$$

where I_{max} and V_{max} are current and voltage limits according to the converter and machine parameters; L is the self-inductance of each phase; M_1, M_2, and M_3 are mutual inductances between one phase and its adjacent and non-adjacent phases of the machine.

In the paper, neglecting the impact of a homopolar voltage component, the value of V_{max} is equal to a half of the DC bus voltage V_{DC} in the Pulse Width Modulation technique. The value of I_{max} can be determined by the peak value of instantaneous currents related to VSI components or the maximum thermal current depending on temperature of windings. According to the machine parameters in Table 1, the verification of the control strategies is carried out with $V_{max} = 100\,V$ and $I_{max} = 7.5\,A$. This value of I_{max} is only for a short-term operation and will decrease in a long-term use according to the thermal constraint of the machine. Operations under and above the base speed (37 rad/s) are analyzed in next sections. Fmincon function in MATLAB is an optimizer that can estimate the parameters of the current references to maximize the torque and respect the constraints on peak values of non-sinusoidal current and voltage.

IV. ANALYSIS OF EFFECTS OF CURRENT PARAMETERS

A. Operation below the base speed

Under the base speed (for example at 20 rad/s), the phase currents are controlled to be maximal (corresponding to a

maximum torque) while the phase voltages are under their limit. The optimal values of the amplitude I_{m1}, ratio k_i and initial phasors (φ_1, φ_3) of the current references are determined by Fmincon and remain unchanged during this operation ($I_{m1} = 8.6\,A$, $k_i = 0.19$, $\varphi_1 = \varphi_3 = 0\,rad$). An analysis using the torque expression (10) to investigate the impacts of the current parameters on the machine torque control will be conducted in this section. For simplicity, only the initial phase angle of the third harmonics φ_3 is considered and denoted by φ while that of the first harmonics is nullified ($\varphi_1 = 0$). In addition, when one of the above parameters of the current references is being considered, the others are constant and equal to their optimal values. Variations of each current parameter (I_{m1}, φ or k_i) within its range and consequent changes in the phase currents and the torque generation at 20 rad/s are derived as follows:

1) Effects of the first harmonic current amplitude (I_{m1})

In the current equations (4-9), I_{m1} is proportional to the peak value of phase currents of the machine. To guarantee the constraint on current, the value of I_{m1} must be less than or equal to the optimal value of 8.6 A which is determined by Fmincon. Besides, the relationships between the average torque, torque ripple and I_{m1} are easily analyzed by using the torque equation (10). When I_{m1} increases from 0 to 10 A, the average torque also linearly rises from 0 to about 70 Nm while the torque ripple value does not change and remains equal to 7.2%. It means that I_{m1} has no effect on the torque ripple but it is proportional to the average torque.

2) Effects of the current phase ($\varphi_3 = \varphi$; $\varphi_1 = 0$)

In Fig. 3, when φ varies within the interval $[-\pi/2; \pi/2]$, enabling sine functions of phase angles in equation (10) to take on their full range of values $[-1; 1]$, the peak value of the non-sinusoidal healthy phase currents varies between 7.5 A and 10.2 A. The lowest peak current is 7.5 A when φ is zero, which means that the constraint on current is satisfied only at that point. Furthermore, the waveform of the currents is also modified. Fig. 4 shows that there are major changes in the torque ripple (from 7% to 63%) but minor variations in the average torque in terms of φ. The optimal value of φ is zero because at this point, the average torque is maximum at 59.6 Nm while the torque pulsation is minimum at 7.2%.

3) Effects of the current ratio (k_i)

The range of the current ratio $k_i = I_{m3}/I_{m1}$ is supposed to increase from 0 to 1. The variation of k_i affects the peak value of phase currents as shown in Fig. 5. The value of k_i must be equal to $k_e = E_{m3}/E_{m1} = 0.19$ so that the peak value of all phase currents is equal to its limit $I_{max} = 7.5\,A$ and the control method MTPA is implemented. In addition, Fig. 6 shows that the torque ripple dramatically increases when k_i varies far away from the value of k_e. The torque average undergoes a moderate increase when k_i gains from 0 to 1.

4) Summary of the functioning under the base speed

From the analyses above, the average torque is sensitive to I_{m1} while the torque ripple is significantly affected by φ and k_i.

It can be seen that $k_i = k_e = 0.19$, $I_{m1} = 8.6\,A$ and $\varphi = 0\,rad$ are the optimal solution of the proposed current references. At these values, the highest average torque equals 59.6 Nm (approximately 80% of the heathy torque as shown in Fig. 11) with a small torque ripple (7.2%) in one opened-phase fault.
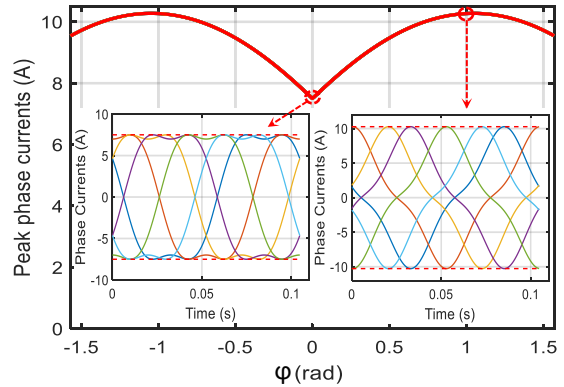

Fig. 3. Effect of $\varphi = \varphi_3$ on the peak value of healthy phase currents when phase *a* is open-circuited and phase current waveforms at $\varphi = 0$ rad and $\varphi = 1$ rad.
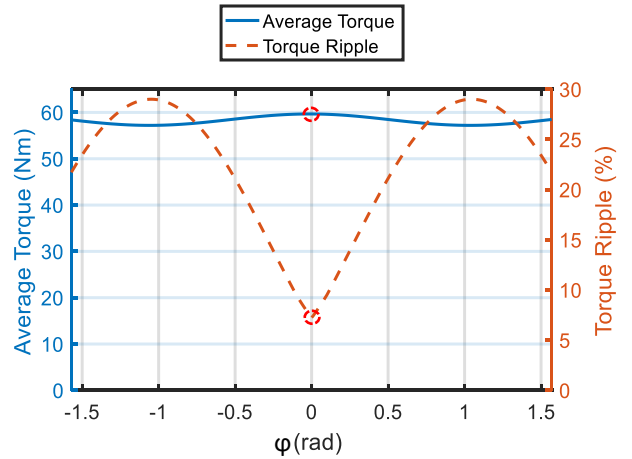

Fig. 4. Impact of $\varphi = \varphi_3$ on the average torque and torque ripple when phase *a* is open-circuited.
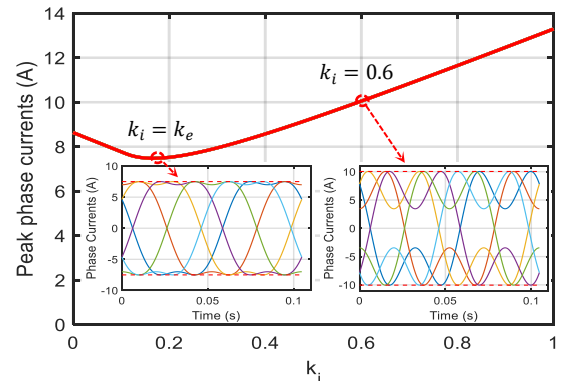

Fig. 5. Effect of $k_i = I_{m3}/I_{m1}$ on the peak value of the healthy phase currents when the phase *a* is open-circuited and, in addition, phase current waveforms at $k_i = k_e = 0.19$ and $k_i = 0.6$.
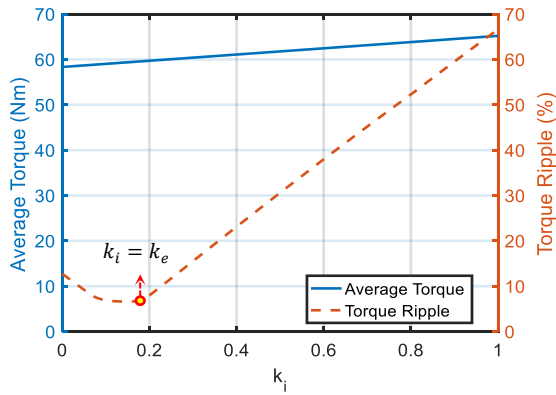
Fig. 6. Impact of $k_i = I_{m3}/I_{m1}$ on the average torque and torque ripple when phase a is open-circuited.

B. The flux-weakening operation

When the speed exceeds the base speed (37 rad/s), the machine turns into the flux-weakening operation. To keep the phase voltages within the constraint value (Fig. 7) and obtain a maximal average torque, the absolute value of the d-axis currents must increase while that of the q-axis currents need to decrease, keeping the peak phase currents equal to I_{max} (Fig. 8). As a result, in natural frame, the first harmonic amplitude I_{m1}, current ratio k_i and initial phases φ_1 and φ_3 of phase currents need to be adapted accordingly at every speed over the base speed. In general, each of the current parameters can be a constant or variable. Because of 4 parameters keeping constant or changing, there are 16 possibilities for the variations of phase currents. However, it is necessary to have at least one adjustable variable among 4 parameters, hence 15 options are available to vary the current parameters to allow the machine to operate in the flux-weakening region. In these options, only cases with variations of φ_1 and φ_3 (for example, strategy 1 as defined in Table 2) can make the peak current value of the healthy phases equal to I_{max} in the flux-weakening operation. In the previous section, it has been shown that parameters φ and k_i affect seriously the peak phase current and the torque ripple. Therefore, strategy 1 produces unacceptable torque ripple increasing from 7.2% under base speed to 60% at 50 rad/s due to adjustments of φ_1 and φ_3 (Fig. 9). Therefore, because I_{m1} has no effect on the torque ripple, a simple solution in which only I_{m1} is varied to respect the voltage constraint and minimize the torque ripple is proposed and named strategy 2 and defined in Table 2. With the strategy 2, the peak value of healthy phase currents changes from I_{max}=7.5A to lower values in the flux-weakening region while their waveforms are identical, for example, the peak value decreases from 7.5 A at 20 rad/s to 2 A at 45 rad/s in Fig. 10. In Fig. 11, the average torques of strategies 1 and 2 are the same under the base speed and equal to 80% of the value in healthy mode. In the flux-weakening region, the torque of the strategy 2 is slightly lower than that of the strategy 1. Nevertheless, in Fig. 12, the torque ripple of strategy 2 at all speeds is tiny and unchanged at 7.2% much smaller than that of strategy 1. These results can be compared with a classical strategy producing no torque ripple: in Figs. 11

and 12, the torque ripple is completely eliminated but the average torque is equal to only 58% of the healthy mode as discussed in [15]. In this strategy, current references in d-q frames are imposed as constant values.

TABLE II. TWO STRATEGIES IN FLUX-WEAKENING OPERATION

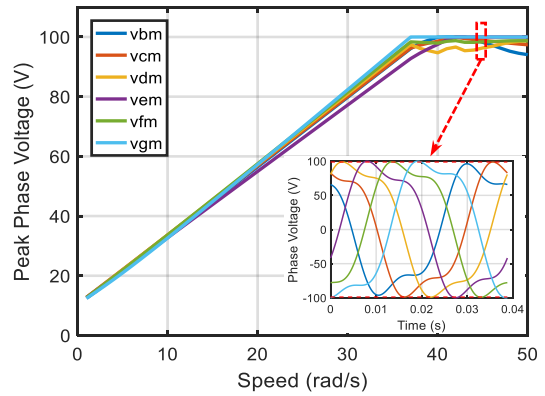| Strategy	I_{m1} (A)	k_i	φ_1 (rad)	φ_3 (rad)
1	variable	variable	variable	variable
2	variable	0.19	0	0

Fig. 7. Voltage-speed characteristics and instantaneous phase voltage at 45 rad/s over the base speed (37 rad/s) when phase a is open-circuited with strategy 1.
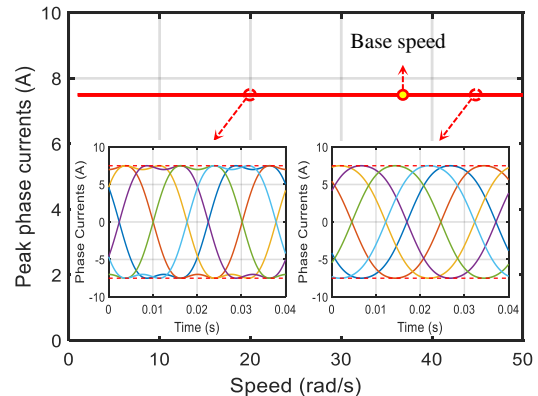

Fig. 8. The peak values of healthy phase currents are unchanged (7.5 A) at speeds over the base speed (37 rad/s) when phase a is open-circuited with strategy 1.
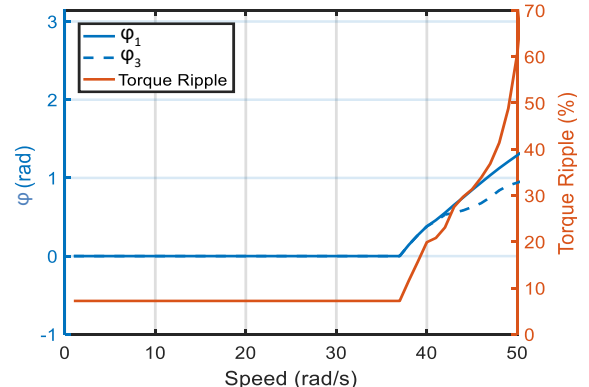

Fig. 9. Initial phases (φ_1,φ_3) and torque ripple when phase a is open-circuited with strategy 1.
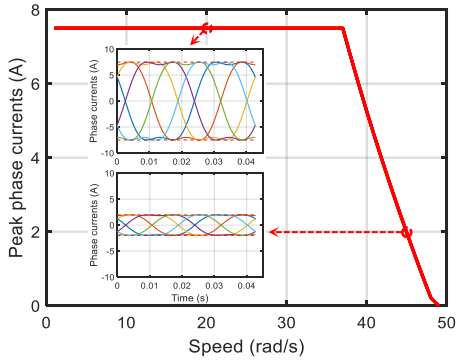
5

Fig. 10. The peak phase currents vs speed and phase currents at 20 rad/s and 45 rad/s (the base speed is 37 rad/s) when phase *a* is open-circuited with strategy 2.
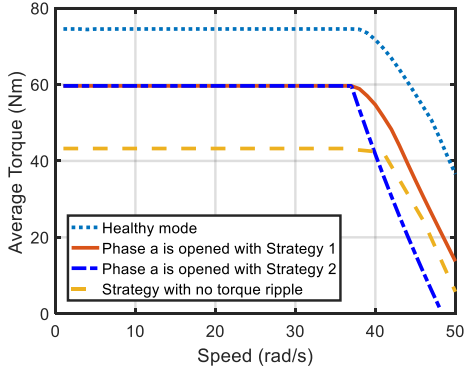

Fig. 11. Average torques in healthy mode and when phase *a* is open-circuited with different strategies.
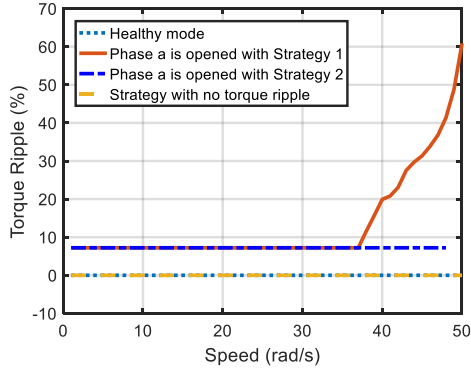

Fig. 12. Torque ripples in healthy mode and when phase *a* is open-circuited with different strategies.

V. CONCLUSIONS

For a 7-phase BLDC machine with non-sinusoidal back-EMFs, the paper has analyzed control strategies imposing two harmonics of phase currents to generate torque and guarantee the constraints on peak values of non-sinusoidal voltage and current. When the torque ripple is not imposed to zero, the proposed current references enable the machine to produce a torque in one-opened phase fault equal to 80% of the heathy torque with a low torque ripple of 7%. On the contrary, if the torque ripple is totally nullified, the average torque probably drops to 58% of the healthy mode. In addition, effects of parameters of the current

references on torque control have been analyzed in the operation under the base speed and in the flux-weakening region. The system is simulated by MATLAB to verify the usefulness of the control strategies. In future, the methods will be implemented to the experimental system.

REFERENCES

[1] E. Levi, "Multiphase Electric Machines for Variable-Speed Applications," *IEEE Transactions on Industrial Electronics,* vol. 55, pp. 1893-1909, 2008.

[2] F. Barrero and M. J. Duran, "Recent Advances in the Design, Modeling, and Control of Multiphase Machines Part I," *IEEE Transactions on Industrial Electronics,* vol. 63, pp. 449-458, 2016.

[3] J. Huang, M. Kang, J. q. Yang, H. b. Jiang, and D. Liu, "Multiphase machine theory and its applications," in *2008 International Conference on Electrical Machines and Systems*, Wuhan, China, 2008, pp. 1-7.

[4] H. A. Toliyat, "Analysis and simulation of five-phase variable-speed induction motor drives under asymmetrical connections," *IEEE Transactions on Power Electronics,* vol. 13, pp. 748-756, 1998.

[5] M. Trabelsi, N. K. Nguyen, and E. Semail, "Real-Time Switches Fault Diagnosis Based on Typical Operating Characteristics of Five-Phase Permanent-Magnetic Synchronous Machines," *IEEE Transactions on Industrial Electronics,* vol. 63, pp. 4683-4694, 2016.

[6] S. Dwari and L. Parsa, "Fault-Tolerant Control of Five-Phase Permanent-Magnet Motors With Trapezoidal Back EMF," *IEEE Transactions on Industrial Electronics,* vol. 58, pp. 476-485, 2011.

[7] A. Mohammadpour and L. Parsa, "A Unified Fault-Tolerant Current Control Approach for Five-Phase PM Motors With Trapezoidal Back EMF Under Different Stator Winding Connections," *IEEE Transactions on Power Electronics,* vol. 28, pp. 3517-3527, 2013.

[8] S. Dwari and L. Parsa, "Open-circuit fault tolerant control of five-phase permanent magnet motors with third-harmonic back-EMF," in *2008 34th Annual Conference of IEEE Industrial Electronics*, 2008, pp. 3114-3119.

[9] F. Locment, E. Semail, and X. Kestelyn, "Vectorial Approach-Based Control of a Seven-Phase Axial Flux Machine Designed for Fault Operation," *IEEE Transactions on Industrial Electronics,* vol. 55, pp. 3682-3691, 2008.

[10] O. Fall, N. K. Nguyen, J. F. Charpentier, P. Letellier, E. Semail, and X. Kestelyn, "Variable speed control of a 5-phase permanent magnet synchronous generator including voltage and current limits in healthy and open-circuited modes," *Electric Power Systems Research,* vol. 140, pp. 507-516, 11/2016.

[11] F. Jen-Ren and T. A. Lipo, "Disturbance-free operation of a multiphase current-regulated motor drive with an opened phase," *IEEE Transactions on Industry Applications,* vol. 30, pp. 1267-1274, 1994.

[12] Z. Sun, J. Wang, G. W. Jewell, and D. Howe, "Enhanced Optimal Torque Control of Fault-Tolerant PM Machine Under Flux-Weakening Operation," *IEEE Transactions on Industrial Electronics,* vol. 57, pp. 344-353, 2010.

[13] F. Locment, E. Semail, and X. Kestelyn, "Optimum use of DC bus by fitting the back-electromotive force of a 7-phase permanent magnet synchronous machine," in *2005 European Conference on Power Electronics and Applications*, 2005, pp.1-9.

[14] F. Locment, E. Semail, and F. Piriou, "Design and study of a multiphase axial-flux machine," *IEEE Transactions on Magnetics,* vol. 42, pp. 1427-1430, 2006.

[15] D. T. Vu, N. K. Nguyen, E. Semail, and T. J. d. S. Moraes, "Torque optimization of seven-phase BLDC machines in normal and degraded modes with constraints on current and voltage," in *The 9th International Conference on Power Electronics, Machines and Drives*, Liverpool, UK, 2018.